Analysis of Impacts Caused by Grid-Connected Photovoltaic System under Varying Conditions

Henrique P. Corrêa[1], **Flávio Henrique T. Vieira**[1]

[1]Escola de Engenharia Elétrica, Mecânica e de Computação, UFG, Goiânia 74605-010, Brazil

henrique19@discente.ufg.br, flavio_vieira@ufg.br

Abstract. *In this paper, we propose a simulation model for grid-connected photovoltaic systems with MPPT control, derived from the photovoltaic cell equivalent circuit. The simulated scenarios aim at reflecting the regular operation of a grid-connected photovoltaic system. The proposed simulation model is validated by comparing its results with theoretical considerations. Since the model is capable of simulating electrical transients during photovoltaic generation, we analyse the photovoltaic generation impacts on the distribution system as a function of typical parameters such as irradiance, temperature, power drained by local load and switching frequency of the inverter.*

Resumo. *No presente trabalho, é proposto um modelo de simulação para sistemas fotovoltaicos conectados à rede com controle MPPT, o qual é derivado a partir do circuito equivalente da célula fotovoltaica. Os cenários simulados objetivam refletir as condições operacionais usualmente encontradas em sistemas interligados. O modelo de simulação proposto é validado por meio da comparação dos resultados obtidos com aqueles calculados via considerações teóricas. Sendo o modelo capaz de simular transitórios elétricos na geração, são analisados nas simulações os impactos da geração fotovoltaica no sistema de distribuição como funções de parâmetros típicos como irradiância, temperatura, potência de carga e frequência de chaveamento do inversor.*

1. Introduction

The growth of distributed generation by means of photovoltaic panels is a global trend verified in power distribution networks. This is justified by rapidly decreasing costs of photovoltaic (PV) systems and the consequent desire of many customers to invest in generating systems that can allow for future energy savings. However, the massive connection of PV panels directly to the distribution grid in the form of grid-connected photovoltaics systems (GCPVS) may cause service problems related to power quality in the distribution grid. For this reason, a large number of recent studies have focused in evaluating the power quality effects as functions of grid characteristics and equipment used in the GCPVS [2,3,6].

Aside from the theoretical characterization of the distribution problems that may occur, an invaluable tool for studying concrete cases of distributed photovoltaic generation is computer simulation. This is of special interest for power utilities and consumers intending to use PV systems, which may require the use of methods that can provide fast estimations of the grid impacts that arise from implementing the GCPVS.

Usually, works regarding the simulation of GCPVS focus on the assessment of grid steady-state conditions as a function of photovoltaic power injection [2,3,6]. However, it may be of interest to apply a dynamic model that allows for the evaluation of electrical transients arising from variable PV generation. In this sense, we propose a simple model for simulating a GCPVS which takes into account grid transients. Considering that most PV systems present short-time transients due to embedded maximum power point tracking (MPPT) systems, we include in our model a controlled DC-DC power converter for simulating and evaluating MPPT performance. The proposed model is implemented in the *Simulink* platform provided by MATLAB.

This work is organized as follows. In Section 2, we present an overview of usual components comprehending a GCPVS and our proposal for modelling the overall system. In Section 3, we validate the MPPT model by simulating a PV system under variable weather conditions feeding a DC load. In Sections 4 and 5, we simulate a GCPVS under nominal and variable weather conditions, respectively. In all simulations, data of a real PV panel is used in order to validate the simulation. The variation of grid impacts as a function of weather conditions and system parameters (inverter type and switching frequency) is discussed. In Section 6, we present conclusions regarding the results obtained in this paper.

2. Modeling of GCPVS

The main components of a GCPVS are PV panel, DC-DC converter controlled by a MPPT algorithm and DC-AC inverter. Additional factors that must be modelled are PV output filters, cable impedance and grid stiffness, which is given by short-circuit capacity at the point of common coupling between PV system and grid. In what follows, the modelling of all these factors will be considered.

2.1. PV Panel

In steady-state simulations of PV panel output, it is reasonable to directly model power as a function of temperature and irradiance. However, the assessment of transient behavior requires that we model the instantaneous voltage-current dependence of the panel. Hence, we opt for using the one-diode model with series resistance, which is depicted in Figure 1 and described by the following equation [7]:

$$I = mV_t \cdot ln\left(\frac{I_{ph} + I_o - I}{I_o}\right) - R_s I \tag{1}$$

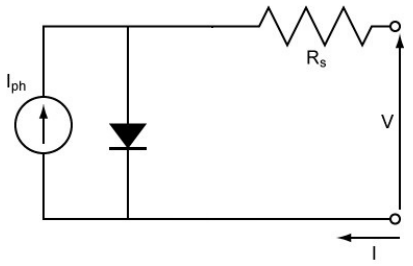

Figura 1. One-diode model with series resistance.

where m is the diode ideality factor, V_t is the termal voltage at $25°C$, I_{ph} is the photogenerated current, I_o is the diode reverse saturation current and R_s is the series resistance.

The values of the equivalent circuit parameters are usually valid for a single irradiance (S) and cell body temperature (T) condition, and can be estimated by using different algorithms in the literature. Furthermore, there exist multiple proposed equations for adjusting the parameter values in order to compensate for non-nominal weather conditions.

In this work, we consider the MSX-60 solar panel in the simulations that follow. The adopted equivalent circuit parameter values are those estimated in [8]. For adjusting voltage and current as functions of temperature and irradiance, we use the following equations given by Buresch et al. [7]:

$$\frac{I_{ph}(T,S)}{I_{ph}(T_o,S_o)} = [1+\gamma_T(T-T_o)]\frac{S}{S_o} \tag{2}$$

$$\frac{V(T,S)}{V(T_o,I_o)} = 1+\beta_T(T-T_o) \tag{3}$$

where (S_o, T_o) is the nominal irradiance and temperature condition, β_T is the open voltage temperature coefficient and γ_T is the short-circuit temperature coefficient.

The above considerations show that simulating dynamic PV panel behavior involves considering both diode non-linearity and current-voltage adjustments in terms of S and T. Considering that it is desirable to simulate transients in real time, an equivalent circuit has to be provided that accounts the mentioned effects. In this sense, we propose the equivalent circuit in Figure 2; the computations used for programming the controlled sources are given in Figure 3.

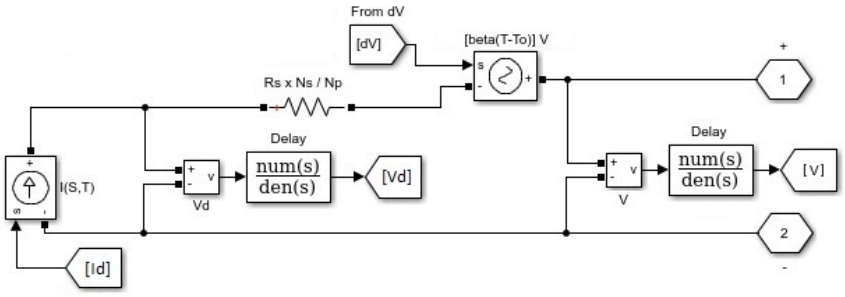

Figura 2. Proposed equivalent circuit for transient simulation.

In Figure 2, V_d and I_d are diode voltage and current, respectively. The diode voltage is measured and used to recalculate I_d according to Equations 1 and 2 while supposing that $R_s = 0$, since the series resistance is considered explicitly in the circuit. The series controlled voltage source has output $\Delta V = \beta_T(T - T_o)V$, which is the voltage increment due to temperature variation. Since these update procedures involve the feedback of voltage values, delay elements (as seen in Figure 2) are used in order to prevent simulation convergence problems. These elements are implemented as simple low-pass filters with a very small time constant $\tau = 10^{-10}$s.

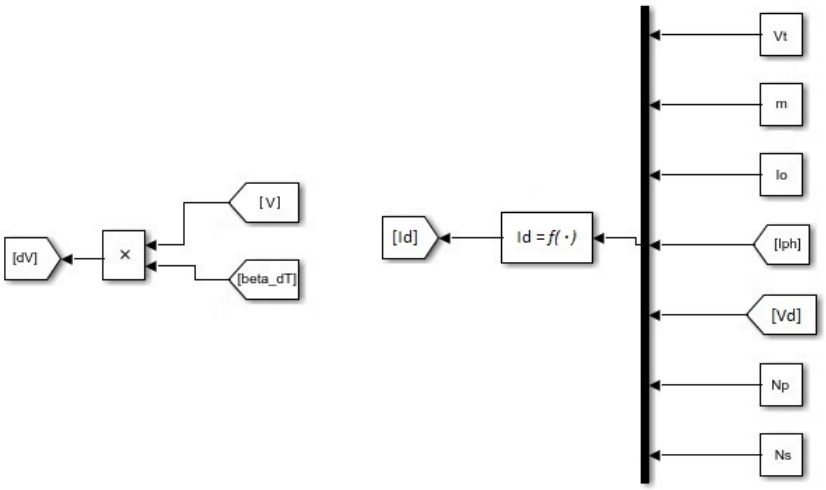

Figura 3. Programming of the controlled sources.

2.2. DC-DC Converter with MPPT

Power electronics DC-DC converters are frequently used in DC systems for regulating voltage output. However, the most common application of these equipment in PV systems is performing MPPT. The basic principle for tracking the panel maximum power point consists in matching the load impedance connected to the panel terminals to its maximum power point impedance $R_{mp} = {}^{V_{mp}}/_{I_{mp}}$, where V_{mp} and I_{mp} are the maximum power point voltage and current.

The converter is switched by a periodic rectangular waveform $s(t)$ with duty cycle $D \in [0, 1]$, which is defined as the ratio between on $(s = 0)$ and off $(s = 1)$ time periods. Depending on the inverter topology, the DC voltage transformation ratio $M = {}^{V_{out}}/_{V_{in}}$ is given as function of the duty cycle $M(D)$. Furthermore, it is known that the impedance transformation ratio is given by $M_Z = {}^{1}/_{M^2}$. Hence, if the load impedance is R, the duty cycle can be controlled in order to make $M_Z \cdot R = R_{mp}$ and attain maximum power extraction from the panel. It must be observed that, in real distribution grids, both R and R_{mp} are variable due to, respectively, grid and weather variations.

In this work, we considered the use of a buck converter for load matching. This topology has a step-down voltage transformation ratio $M(D) = D$ and is adequate for matching sources connected to relatively high impedances, since $M_Z(D) \geq 1$. Considering that the power grid usually presents inductive impedances connected to the generation bus, the transmitted power may be weakly influenced by voltage, which implies in a high impedance for the DC system. Hence, the use of a buck converter is justified.

We choose as the MPPT control algorithm the Perturb and Observe (P&O) method, which is the most regularly used in PV systems due to its simplicity and effectiveness [1]. Its principle consists in periodically perturbing the current duty cycle by an increment ΔD and assessing the corresponding change in output power. Depending on the power variation, the sign of ΔD may be mantained or switched. This procedure enables the system to track the panel variable maximum power point due to changing weather. The converter topology is given in Figure 4, where the voltage and current mea-

surements are used as feedback for evaluating output power. Adopted system parameters are $C = C_{in} = 1mF$ and $L = 10mH$, which restricts inductor current ripple under 100 mA for $D = 1$ and filters the high-order harmonics.

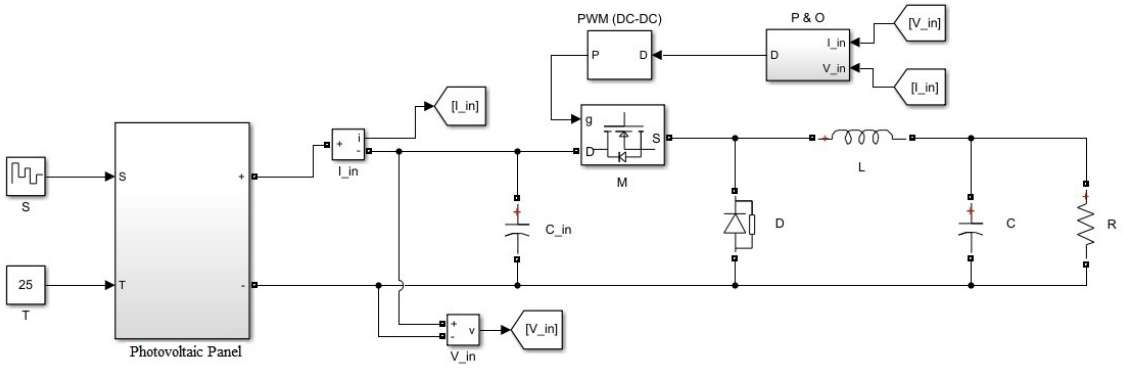

Figura 4. Buck converter with MPPT control.

2.3. Inverter and Grid Interface

In most GCPVS, the DC-DC converter output is directly connected to the input terminals of the DC-AC inverter, which can have a single or three-phase topology. The AC voltage output contains significant harmonic content due to the nonlinear operation of the inverter; aditionally, the spectral distribution is dependent on the switching strategy for controlling the inverter. In this work, we consider a three-phase inverter that may be controlled by two different switching methods, namely square-wave and PWM switching. These methods were chosen because they are the most commonly applied in real systems. The inverter line-to-line voltages at grid frequency are:

$$V_{PWM} = \frac{\sqrt{3}}{2\sqrt{2}} m_a V_d \tag{4}$$

$$V_{square} = \frac{\sqrt{6}}{\pi} V_d \tag{5}$$

where V_d is the input DC voltage and m_a is the PWM amplitude modulation index [4], for which we assume $m_a = 1$.

For the simulated system, we consider the association of sixty MSX-60 panels in the form of six parallel strings with ten panels each, which at maximum power and supposing $D = 1$ yields $P_{mp} \approx 3.6kW$ and $V_{PWM} \approx 100V$. Hence, we consider that the inverter is connected to the grid via a step-up transformer with $100V : 380V$ voltage transformation ratio.

Aside from the inverter model, the output filter for harmonic attenuation must be considered. We consider for our model the usual LC filter topology, with the inductor $(L = 10mH)$ and capacitor $(C = 50\mu F)$ being placed in the low and high-voltage side of the transformer, respectively. These values are chosen in order to achieve a filter cutoff frequency of approximately 120 Hz.

Finally, we model the local load as an RL series impedance with power factor 0.92 and nominal apparent power equal to $1kVA$. The load values were chosen in order to match the PV system nominal power. The grid is modelled as a Thévenin equivalent given by $\hat{V_{th}} = 220\angle 0°$ and $Z_{th} = 0.5 + j0.3\Omega$ at 60 Hz. The selected Z_{th} represents usual grid impedance values as seen from low-voltage consumer buses [5].

In order to allow the maximum power transfer to the grid, power flow equations [5] can be used together with the filter inductance value to show that the inverter voltage phase must be approximately $\delta = 90°$. With this value of phase and considering the filter capacitor compensation, the expected reactive power was calculated as $Q = -333Var$. The inverter and grid model is given in Figure 5.

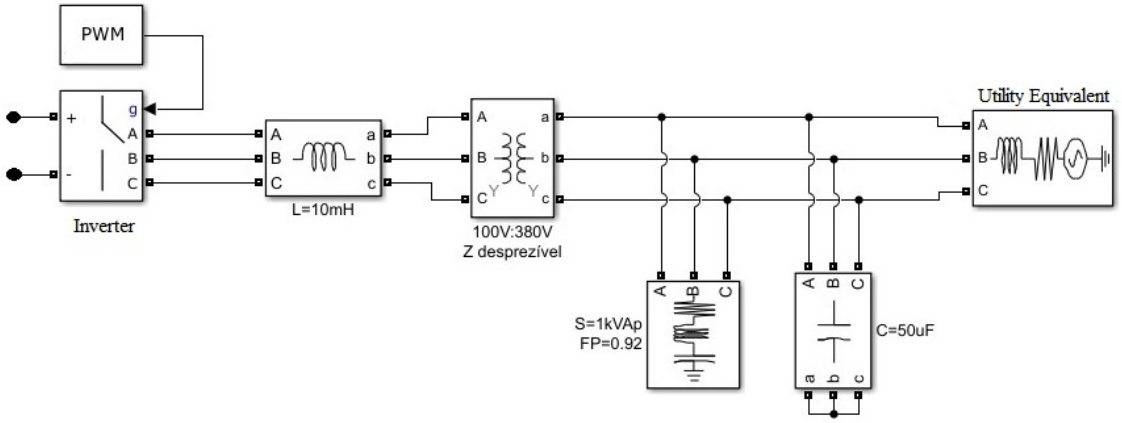

Figura 5. Inverter and power grid model.

3. Validation of MPPT Controller Model

The equivalent resistance represented by the distribution network is high when compared to the equivalent maximum power resistance R_{mp} of the photovoltaic panel, which can vary widely as a function of the environmental conditions. As an example, with the supplied current being practically proportional to the irradiance, a given increase in S implies a reduction in R_{mp} by the same factor. In this context, therefore, it is enough to verify the proper operation of the load matching for variations in environmental conditions, assuming a fixed large-resistance DC load imposed to the panel.

Hence, we arbitrate the connection of a resistive load $R = R_{mp}|_{STC} \approx 4.88\Omega$ to the panel terminals. Thus, for a nominal irradiance $S = 1000W/m^2$, the load matching must occur with $D = 1$. In order to demonstrate the transient behavior of the MPPT algorithm, we started the simulation with nominal irradiance and duty cycle $D = 0.1$.

The literature indicates that MPPT control stability is strongly dependent on the sampling frequency f_{MPPT} and on the ΔD increase [1]. In particular, it is considered that defining $f_{MPPT} = 1Hz$ and $\Delta D = 0.1$ is enough to assure stability. The increases in sampling frequency and/or reductions in duty cycle increments must be tested to confirm a stable operation [1]. By means of preliminary simulations, we noticed that the dynamics of the system comprising a buck converter and the load R is such that $f_{MPPT} = 5Hz$ and $\Delta D = 0.1$ are stable control parameters. We changed the irradiance in 1.5 s steps by means of a cyclic sequence $S = \{1000, 500, 800, 300, 600, 1000, 500, ...\}W/m^2$.

By simulating the system in accordance with previous considerations, we obtained the results shown in Figures 6 to 8. The graphs correspond, respectively, to the dynamic variations in power, duty cycle, and efficiency over the course of system operation. Figure 6 shows an auxiliary curve indicating the maximum power that can be extracted at the current irradiance level. The system efficiency is calculated as the ratio between supplied power and the current maximum power level.

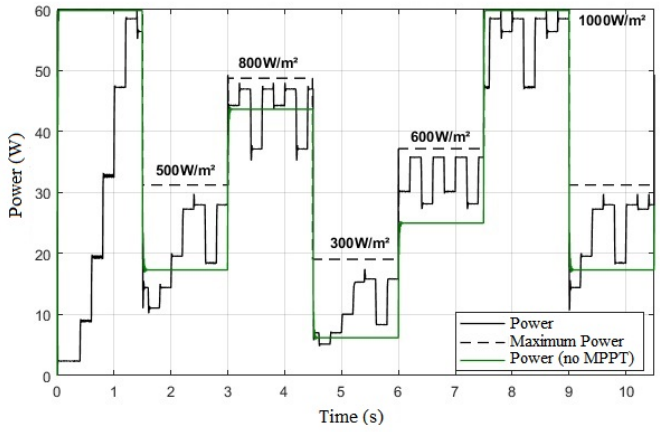

Figura 6. Dynamic variation of supplied power (variable S).

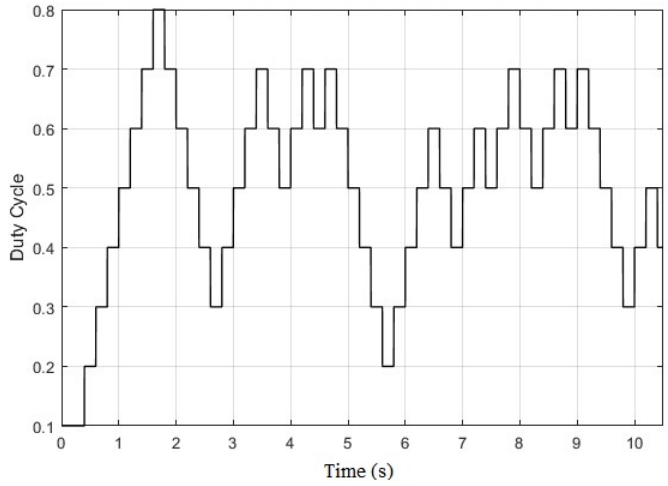

Figura 7. Dynamic variation of duty cycle (variable S).

The simulation results demonstrate the expected behavior for the P&O algorithm. The system, through duty cycle adjustments for different irradiances, always tends to operational regions near the maximum power point. In addition, short three-level operation intervals are observed, which is an indication that the algorithm stabilizes around the maximum power current value P_{mp}.

Another outstanding characteristic of the system is its ability to adjust relatively quickly to abrupt shifts in irradiance. This becomes visible by the transient process when the system starts up with $D = 0.1$. In a nearly one second time interval, the system

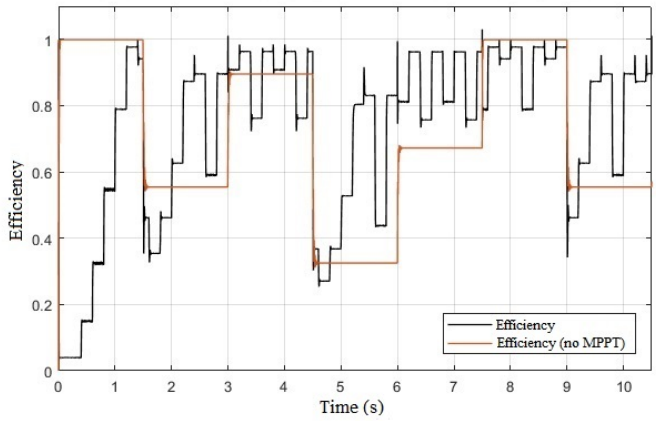

Figura 8. Dynamic variation of efficiency (variable S).

reaches the region near the maximum power point. Finally, we note that, in the intervals of supplied power stabilization, the average efficiency of the system lies in the neighborhood of $\eta = 85\%$. This could possibly be optimized by decreasing ΔD, at the cost of lower stability.

The verified power levels corroborate the proposed photovoltaic model. It is known that the maximum output power varies almost linearly with the incident irradiance; in Figure 6, it is immediately understood that this second relation is met in the simulation.

To check the load matching system capacity in changing temperatures, the procedures of the previous simulation were repeated. The only modification was keeping the irradiance at its $1000W/m^2$ nominal value and varying the body temperature in steps. The configuration parameters of the MPPT algorithm remained the same, as well as the 1.5 s time for the different temperature levels. The chosen cyclic sequence for the temperature steps is expressed by $T = \{25°C, 75°C, 50°C, 100°C, 85°C, 25°C, 75°C, ...\}$.

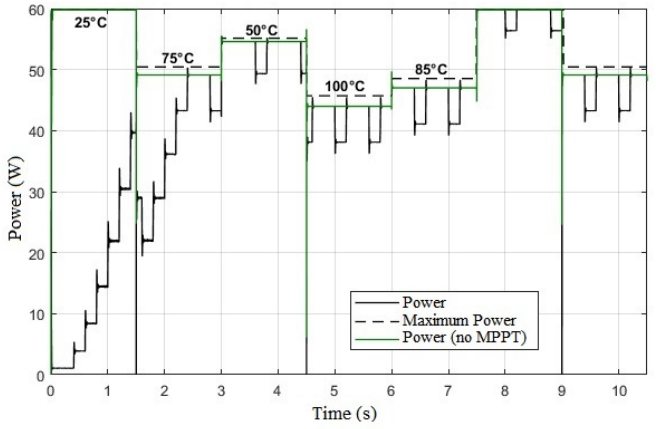

Figura 9. Dynamic variation of supplied power (variable T).

Again, the results are consistent with the theoretically expected values. It is possible to notice that the temperature influences the converter load matching less significantly

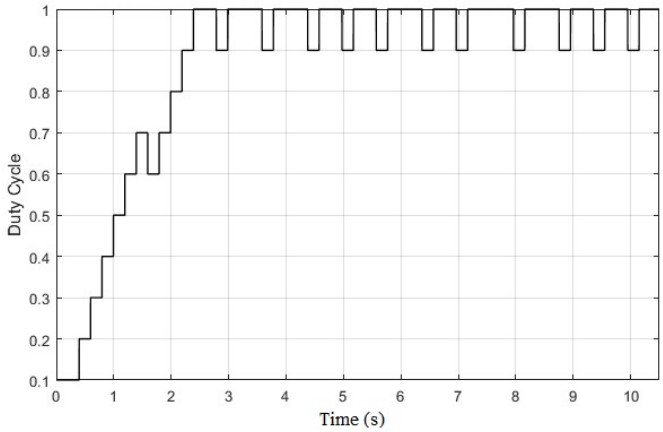

Figura 10. Dynamic variation of duty cycle (variable T).

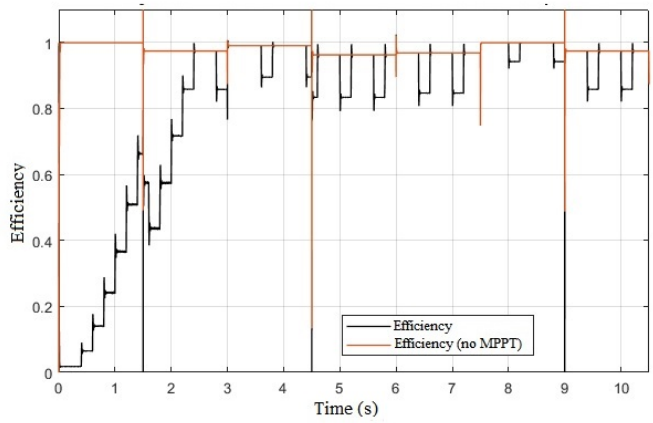

Figura 11. Dynamic variation of efficiency (variable T).

than the irradiance. In fact, Figures 9 to 11 display the system stabilization around $D = 1$, independently of T. This indicates that the panel maximum power equivalent resistance (R_{mp}) is not sufficiently changed by the temperature for the system to compensate for impedance matching. However, although the duty cycle remains in the same range for various temperatures, the operation always occurs close to the maximum power.

To briefly summarize, the load matching by the converter is strongly dependent on irradiance and the equivalent impedance value represented by the load itself imposed on the photovoltaic panel. On the other hand, dependence on temperature is small; a scenario in which only T will imply small variations in the duty cycle stabilization range, especially if ΔD is large.

Finally, we observed that the maximum power levels shown in Figure 9 are consistent with those calculated by the Buresch et al. [7] method. It is interesting to note that, in the case of varying temperature with a matched load under nominal conditions, the MPPT system tends to reduce the efficiency value. This is explained by the fact that, without the use of MPPT, the load would remain approximately matched for all temperatures.

4. GCPVS Operation under Nominal Conditions

The photovoltaic system connected to the distribution network was designed based on its operation under nominal environmental conditions (STC). To facilitate the comparison process with the design parameters, we chose to simulate the photovoltaic system operating under constant and nominal environmental conditions.

The presence of the LC output filter contributes to an increase in photovoltaic system accommodation time, creating the need to reduce the frequency f_{MPPT} in relation to the frequency used in the previous section. By means of preliminary simulations, we identified the stable operation of the MPPT controller for $f_{MPPT} = 1Hz$ and $\Delta D = 0.1$. The simulated circuit parameters correspond to those previously designed.

The system was simulated for inverter operation in pulse width modulation (PWM) $(m_a = 1)$ and square-wave. We noticed that the duty cycle and the active and reactive power behaviors in the fundamental frequency were identical. However, the harmonic distortion of the current injected into the network was significantly higher for the square-wave operation. Figures 12 to 14 correspond, respectively, to the graphs of active and reactive power, and duty cycle observed in steady state operation.

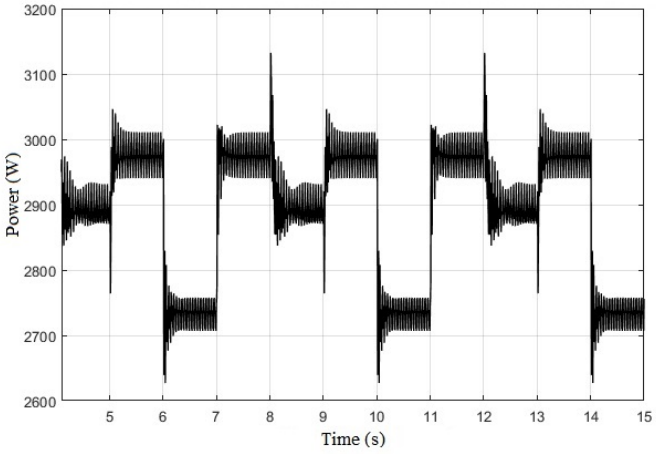

Figura 12. Active power in MPPT steady state.

The results presented in these figures are in line with the design of the reference photovoltaic system. Considering the average value of MPPT efficiency in the previous section, $\eta \approx 85\%$, we estimated an average active power $P_{avg} \approx 3060W$. This value is in accordance with Figure 12. Nevertheless, the system was designed to provide a reactive power $Q = 333Var$; Figure 13 shows that the results are close to this value. Finally, the design of the LC output filter inductance, so that the system drains the panel nominal power, suggested that the duty cycle oscillation would be close to one, which can be seen in Figure 14.

The voltage and current ripples in the buck converter for the operation with $D = 0.8$. Considering that this duty cycle value occurred in the simulation, the ripple values were determined for the intervals with $D = 0.8$ and compared with the theoretical values. The results are shown in Table 1.

Finally, Figures 15 and 16, respectively, display the waveforms of the current sup-

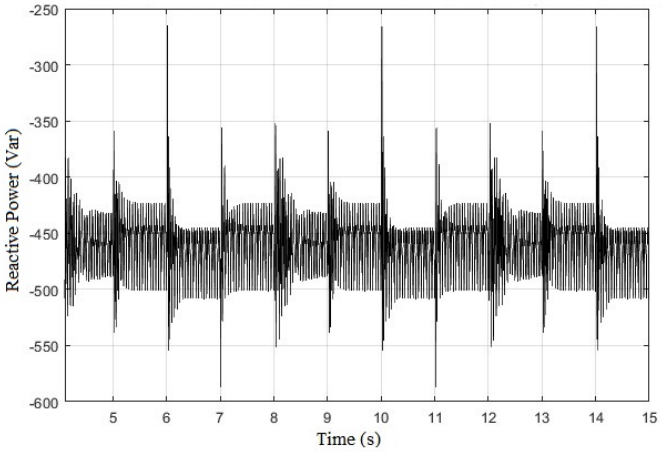

Figura 13. Reactive power in MPPT steady state.

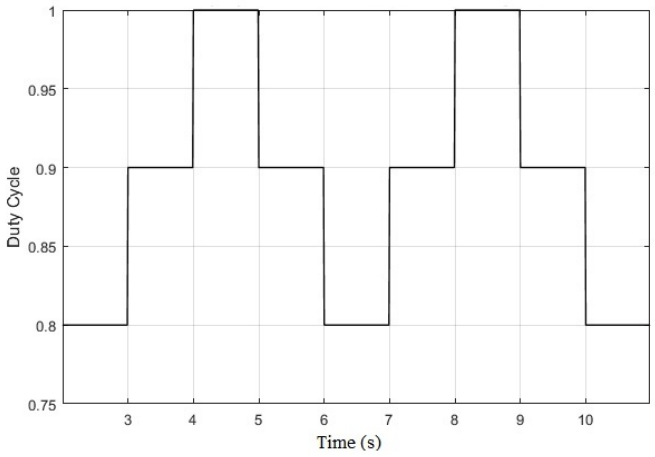

Figura 14. Steady state MPPT duty cycle.

Tabela 1. Values of *ripple* for $D = 0.8$.

Ripple	Theoretical Value	Simulated Value
ΔI_L	$85mA$	$70mA$
ΔV_o	$2.7mV$	$2.3mV$

plied by the photovoltaic system for square-wave and PWM operations. The associated THD (Total Harmonic Distortion) values are listed in Table 2.

Tabela 2. Output current THD values.

Operation Mode	THD_I
PWM	0.77%
Square-Wave	8.66%

The results highlight that the supplied current waveform in the square-wave operation shows considerable levels of harmonic distortion. Nevertheless, the LC filter seen in the present simulation is significantly stronger than those found in practical applicati-

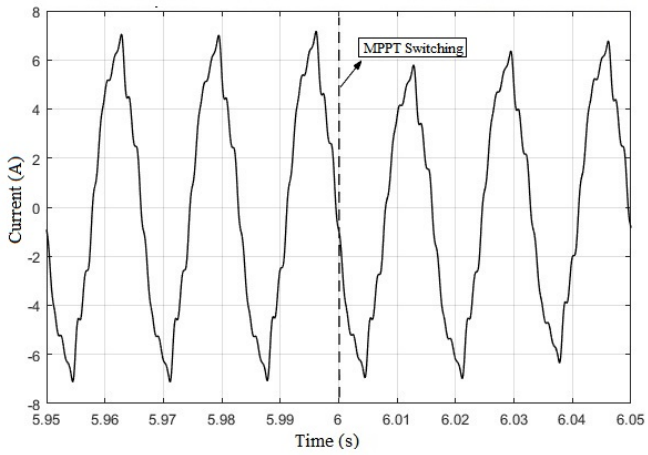

Figura 15. Injected current for square-wave operation.

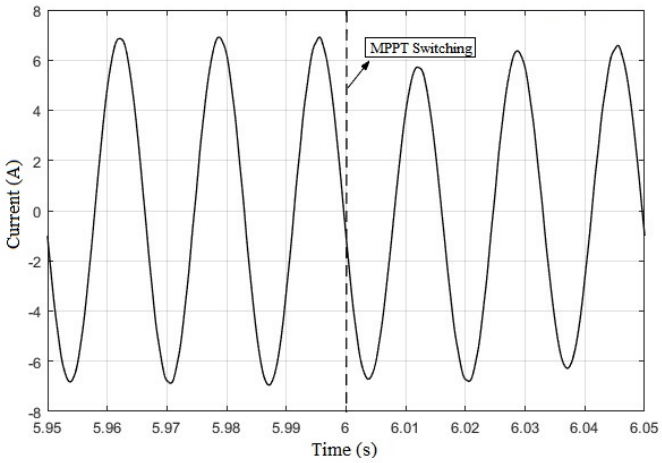

Figura 16. Injected current for PWM operation.

ons, considering that the implementation of filters with low cut-off frequencies is costly. Therefore, in practice, the THD of the supplied line current is bound to be even greater than that obtained in this study.

On the other hand, the obtained current in the PWM mode simulation is, virtually, a sine wave. It is possible to state that the used cut-off frequency is characterized as an over-dimensioning of the LC filter for the PWM operation, keeping in mind that significant harmonic frequencies are in $f \geq 8kHz$. This result demonstrates that it is possible to implement satisfactory energy quality at affordable costs, considering that harmonic filtering will not require the use of robust and therefore costly filters. These considerations justify the commercial designation of PWM inverters as pure sine wave inverters.

5. GCPVS Operation under Varying Conditions

In this section, we intend to briefly illustrate, by application of the proposed simulation model, the variations in photovoltaic generation impact on the distribution system as a function of typical parameters such as irradiance, temperature, power drained by local load, and switching frequency of the inverter (f_s).

The comparisons were defined by conducting simulations similar to those in the previous section, in which the pertinent parameters were individually modified. The considered scenarios, whose results are in Tables 3 to 6, were as follows:

- Varying irradiance: nominal value, $S_1 = 600W/m^2$ and $S_2 = 300W/m^2$.
- Varying temperature: nominal value, $T_1 = 0°C$ and $T_2 = 50°C$.
- Varying load: nominal value, $S_1 = 3kVA$ and $S_2 = 10kVA$.
- Varying PWM frequency: nominal value, $f_{s,1} = 1kHz$ and $f_{s,2} = 16kHz$.

Tabela 3. Obtained values for variable irradiance.

Parameter	$S = 1000W/m^2$	$S = 600W/m^2$	$S = 300W/m^2$
V	$381.5V$	$379.7V$	$378.3V$
THD_V	0.46%	0.27%	0.13%
I	$4.88A$	$3.11A$	$1.62A$
THD_I	8.66%	8.66%	8.64%
$(P/Q)_{carga}$	$1008W/429Var$	$998W/425Var$	$991W/422Var$
$(P/Q)_{PV}$	$2900W/-700Var$	$1450W/-800Var$	$470W/-825Var$

Tabela 4. Obtained values for variable temperature.

Parameter	$T = 25°C$	$T = 0°C$	$T = 50°C$
V	$381.5V$	$381.9V$	$381.1V$
THD_V	0.46%	0.51%	0.43%
I	$4.88A$	$4.93A$	$4.22A$
THD_I	8.66%	8.65%	8.66%
$(P/Q)_{carga}$	$1008W/429Var$	$1010W/430Var$	$1006W/428Var$
$(P/Q)_{PV}$	$2900W/-700Var$	$3150W/-710Var$	$2520W/-750Var$

Tabela 5. Obtained values for variable load.

Parameter	$S_{carga} = 1kVA$	$S_{carga} = 3kVA$	$S_{carga} = 10kVA$
V	$381.5V$	$378.2V$	$367.2V$
THD_V	0.46%	0.46%	0.43%
I	$4.88A$	$4.51A$	$4.47A$
THD_I	8.66%	8.66%	8.66%
$(P/Q)_{carga}$	$1008W/429Var$	$2970W/1266Var$	$9340W/3978Var$
$(P/Q)_{PV}$	$2900W/-700Var$	$2820W/-740Var$	$2750W/-680Var$

The results show that a major parameter influencing power supplied by the system is irradiance; the photovoltaic power is practically proportional to the irradiance level S. On the other hand, temperature is less critical to the generation; however, its effect cannot be neglected because the trend in photovoltaic installations is the heating of panels to levels significantly higher temperatures than the local room temperature, leading to a decrease in supplied power. For the inverter operation in PWM mode, the current harmonic distortion strongly depends on f_s. The utilization of values far above the cut-off frequency fosters the THD_I reduction to negligible levels. However, the use of small f_s may result in distortion levels even higher than the ones found in square-wave modulation.

Tabela 6. Obtained values for variable f_s.

Parameter	$f_s = 8kHz$	$f_s = 1kHz$	$f_s = 16kHz$
V	$381.5V$	$381.4V$	$381.5V$
THD_V	0.04%	0.8%	0.03%
I	$4.88A$	$4.88A$	$4.88A$
THD_I	0.77%	10.36%	0.21%
$(P/Q)_{carga}$	$1008W/429Var$	$1006W/429Var$	$1008W/419Var$
$(P/Q)_{PV}$	$2900W/-700Var$	$2895W/-702Var$	$2901W/-700Var$

6. Conclusion

A photovoltaic panel model capable of simulating electrical transients has been proposed. The model was validated via simulation of two common scenarios for PV power generation, namely MPPT tracking of a variable load and assessment of grid-connected PV system power quality impacts as a function of weather conditions and system parameters. The obtained results show that the proposed model reliably reproduces the transient phenomena associated with MPPT and inverter switchings, providing accurate generated power and harmonic distortion values. The computational experiments have also shown that the model can be used in order to obtain time plots of system variables (e.g. power, current and duty cycle), which is an advantage over steady-state models.

References

1. M. Elgendy, B. Zahawi, D. Atkinson, Assessment of perturb and observe mppt algorithm implementation techniques for pv pumping applications, IEEE Transactions on Sustainable Energy.

2. R. A. Shayani, Método para a determinação do limite de penetração da geração distribuída fotovoltaica em redes radiais de distribuição, Ph.D. thesis, Universidade de Brasília (2010).

3. A. A. Latheef, Harmonic impact of photovoltaic inverter systems on low and medium voltage distribution systems, Master's thesis, University of Wollongong (2006).

4. N. Mohan, T. Undeland, Power electronics: converters, applications, and design. Wiley India, 2007. ISBN 9788126510900.

5. W. Stevenson, Elements of power system analysis, McGraw-Hill series in electrical engineering: Power and energy, McGraw-Hill, 1982.

6. R. A. Kordkheili, B. Bak-Jensen, J. R-Pillai, P. Mahat, Determining maximum photovoltaic penetration in a distribution grid considering grid operation limits, in: 2014 IEEE PES General Meeting, 2014.

7. M. Buresch, Photovoltaic energy systems: design and installation. McGraw-Hill, 1983. ISBN 9780070089525.

8. M. G. Villalva, J.R. Gazoli, E. R. Filho. Comprehensive approach to modeling and simulation of photovoltaic arrays. IEEE Transactions on Power Electronics, 2009.